Mechanical Systems and Signal Processing 38 (2013) 585–600

Contents lists available at SciVerse ScienceDirect

Mechanical Systems and Signal Processing

journal homepage: www.elsevier.com/locate/ymssp

The loss factor experimental characterisation of the non-obstructive particles damping approach

M. Ben Romdhane [a,*], N. Bouhaddi [b], M. Trigui [a], E. Foltête [b], M. Haddar [a]

[a] Mechanics, Modelling and Manufacturing Research Unit, National School of Engineers of Sfax BP 1173, 3038 Sfax, Tunisia
[b] Department of Applied Mechanics, FEMTO-ST Institute, UMR 6174, 24 Chemin de l'Epitaphe, 25000 Besançon, France

ARTICLE INFO

Article history:
Received 5 May 2012
Received in revised form
20 December 2012
Accepted 6 February 2013
Available online 6 March 2013

Keywords:
Granular material
Passive damping
Energy dissipation
Friction
Loss factor

ABSTRACT

The Non-obstructive Particle Damping (NOPD) technology is an actuality research topic in vibration attenuation. In spite of the simplicity of this technology, the large number of NOPD parameters constitutes one of the problems in the computation of its damping contribution. In this paper, an experimental characterisation of non-obstructive particle damper under harmonic excitation was investigated. The experimental method which was developed allows the quantification of NOPD's loss factor independently of the structure. Some system parameters such as excitation frequencies, excitation amplitudes and geometry of granular cavity were examined. Afterward, the characterised damping was converted to an equivalent viscous damping in order to predict the dynamic behaviour of a damped structure. The good correlation between experimental and numerical results illustrates the performance and the usefulness of the proposed method.

1. Introduction

Non-Obstructive Particle Damping (NOPD) technology is a passive vibration damping approach used to absorb vibration energy. It consists of making small diameter holes or cavities at appropriate locations inside vibrating structures. These holes are filled to appropriate levels with metallic or non-metallic [1] particles in spherical form which yields the maximum damping effectiveness for the desired mode. The major energy dissipation mechanisms of granular particles are related to friction [2,3] and impact [4–7] phenomena which are highly non-linear.

Due to its conceptual simplicity and low cost, this passive damping concept has been used successfully in many fields (shuttle space [8], turbine blades [9] and industrial machine [11]) to reduce vibration. In addition, the NOPD passive damping approach can operate in extreme temperature conditions when using a metallic, tungsten carbide or ceramic particle which is not the case of viscoelastic materials.

The granular particle aspect, allowing interactions between grains and container walls, is the subject of a lot of research ([10–15]). As an example, Xu et al. [3] developed physical models to take into account the shear frictional forces between particle layers. The authors also performed experimental tests of the beam and plate structures for various damping treatments. As another way to estimate the performance of the particle damper, Liu et al. [13] converted the damping contribution of NOPD to an equivalent linear viscous damping. The effectiveness of NOPD is determined by analysing the

* Corresponding author. Tel.: +33 3 81 66 60 56; fax: +33 3 81 66 67 00.
E-mail address: benromdhanemanel@yahoo.fr (M. Ben Romdhane).

0888-3270/$ - see front matter © 2013 Elsevier Ltd. All rights reserved.
http://dx.doi.org/10.1016/j.ymssp.2013.02.006

frequency response of a single degree of freedom system. It is noticed that most of the previous investigations characterise the performance of the NOPD by the use of a primary structure.

Based on extensive experimental results, Lenzi [10] developed an approximate method to predict the damping achieved by a beam filled with granular materials. In the complexity of the dynamic behaviour of granular materials, the parameters referred to here are amplitudes of vibration, pressure, grain sizes, and dimension of cavities and frequency of vibration.

Despite the simplicity of this technology, the characterisation of NOPD is still complicated (the complexity interactions in the particle damper). Besides, most of this research is based on experimental investigation. In fact, several parameters affect the damper performance, such as pressure, particle size, compaction, the internal design of the enclosure, excitation level and frequency band of interest. In particular, the internal design of the enclosure [13] and the quantity of granular material [10] are the most important parameters.

The close dependence of the energy dissipation phenomenon on several parameters has led us to develop an original approach in reference to literature studies. This approach consists in proposing an experimental method to characterise the NOPD loss factor independently of mechanical structure. The basic idea of this experimental method is to determine the total power and the dissipated power during the vibration damper. This approach, used by Yang [16] to characterise the damping effect of granular materials, is based on the power flow method which was introduced by Fourier.

In this work, an experimental procedure was developed for a series of design dampers in order to measure the loss factor of the non-obstructive particle dampers. A parametric study was used to describe the nonlinear characteristics of the NOPD. Then the characterised damping was converted into an equivalent linear viscous damping coefficient depending on frequency that can be easily introduced in a predicted model. In the second part, a numerical study of a beam treated with NOPD was performed. Its purpose was to predict the dynamic behaviour of a primary structure using the loss factor characterised by power measurements. An experimental study was conducted to check the capacity of this method to predict the contribution of NOPD in the damping of a primary structure.

2. Experimental characterisation of non-obstructive particles damper

The Non-obstructive Particle Damper characterised in this study is a non-deformable cylindrical enclosure filled with granular material (Fig. 1). Thanks to a swept-sine excitation provided by an electromagnetic shaker, the variation of both force and velocity of the damper versus frequencies was measured. Afterwards, the measured quantities were used in the computation of the NOPD's loss factor. The measurement technique of the loss factor is presented in the next section.

2.1. Loss factor measurements technique

In order to measure the power dissipation energy conducted on the enclosure we used the method chosen by Yang to characterise particle dampers. This theory is based on the Fourier-based power flow method. Basically, the work done in a

Fig. 1. Cylindrical enclosure.

cycle to excite a mass is given as [17]

$$W_{cycle} = \int_0^T f(t)v(t)dt \tag{1}$$

where $f(t)$ and $v(t)$ are the force and velocity, respectively, and T is the length of one cycle. The term $f(t)\ v(t)$ denotes the instantaneous power. Then the average power transmitted is therefore given as

$$P_{av} = \frac{W_{cycle}}{T} = \frac{1}{T}\int_0^T f(t)v(t)dt \tag{2}$$

The representation of the force and velocity data set as a complex Fourier series in a discrete manner can be given by the following equation:

$$P_c = \frac{1}{T}\int_0^T \left(\sum_{n=0}^{\infty} f_n e^{j(n\omega t-\varphi_{Fn})}\right)\left(\sum_{m=0}^{\infty} v_m e^{j(m\omega t-\varphi_{vm})}\right)dt \tag{3}$$

where

- P_c is the complex power;
- f_n and v_m are the magnitudes of the force and velocity of the nth and mth harmonic, respectively;
- φ_{Fn} and φ_{vm} are the phases of the force and velocity of the nth and mth harmonic, respectively.

The integrals between all cross-terms cancel out:

$$P_c = \frac{1}{2}\sum_{n=0}^{\infty} f_n v_n e^{j(\varphi_{Fn}-\varphi_{vn})} \tag{4}$$

Basically, the complex power associated to one harmonic cycle is expressed as

$$P = F_{rms}V^*_{rms} \tag{5}$$

where F_{rms} and V^*_{rms} are respectively the complex force and conjugate of the complex velocity.

The real part of power Re $al\{P\}$ also known as "active power" represents the dissipated power provided by the granular material motions.

$$\mathrm{Re}al\{P\} = F_{rms}V_{rms}\cos(\varphi_F-\varphi_V) \tag{6}$$

where $(\phi_F-\phi_V)$ is the phase difference between the force and velocity signals in radians.

The imaginary part of power Im$ag\{P\}$ also known as "reactive power" is the trapped power. This power can be expressed as follows:

$$\mathrm{Im}ag\{P\} = F_{rms}V_{rms}\sin(\varphi_F-\varphi_V) \tag{7}$$

Thus, the definition of NOPD loss factor is given as [17]

$$\eta = \frac{E_{dissipated}}{E_{\max\ imum}} = \frac{\mathrm{Re}al\{P\}}{\mathrm{Im}ag\{P\}} \tag{8}$$

where $E_{dissipated}$ is the amount of dissipated energy in a cycle per radian, and $E_{\max\ imum}$is the maximum energy stored in a cycle.

2.2. Experimental descriptions

The experimental arrangement is shown in Figs. 2 and 3. The non-obstructive particle damper represents a cylindrical aluminium enclosure closed with a cover and fixed to electromagnetic shaker. To guarantee a better fixation of the cover and the enclosure ceiling, four screws were used. The design of the cylindrical enclosure allows it to acquire a rigid behaviour in the frequency band of analysis. The total mass of steel particles having 0.5 mm diameter was 52 g. The measurement of the velocity and force were assured respectively by a laser vibrometer and a force sensor was placed between the enclosure and the shaker. A multichannel dynamic signal analyser SIGLAB model 20-42 was used to collect and process the data. The advantage of this arrangement is to measure both force and velocity without contact with the structure.

The experimental process was organised in two steps:

In the first step, a series of measurements was conducted with an empty enclosure. The goal of this set of tests was to check the computation of powers; this included the analysis and calibration of the experiment parameters which had an effect on the measurement precision.

In the second step, steel particles were placed inside the enclosure and compacted by the cover through four screws. The measurements of force and velocity were performed taking into account the instrument calibration done using the

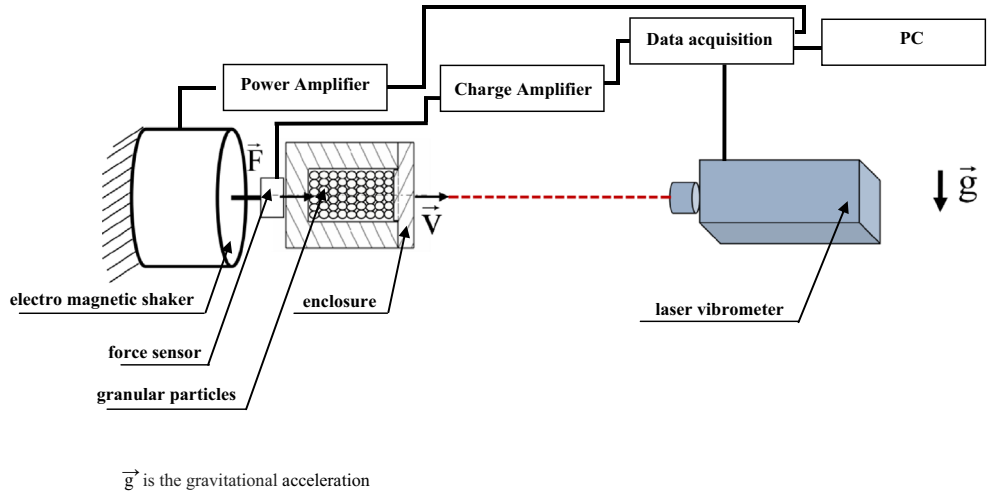

Fig. 2. Schematic of loss factor measurement setup.

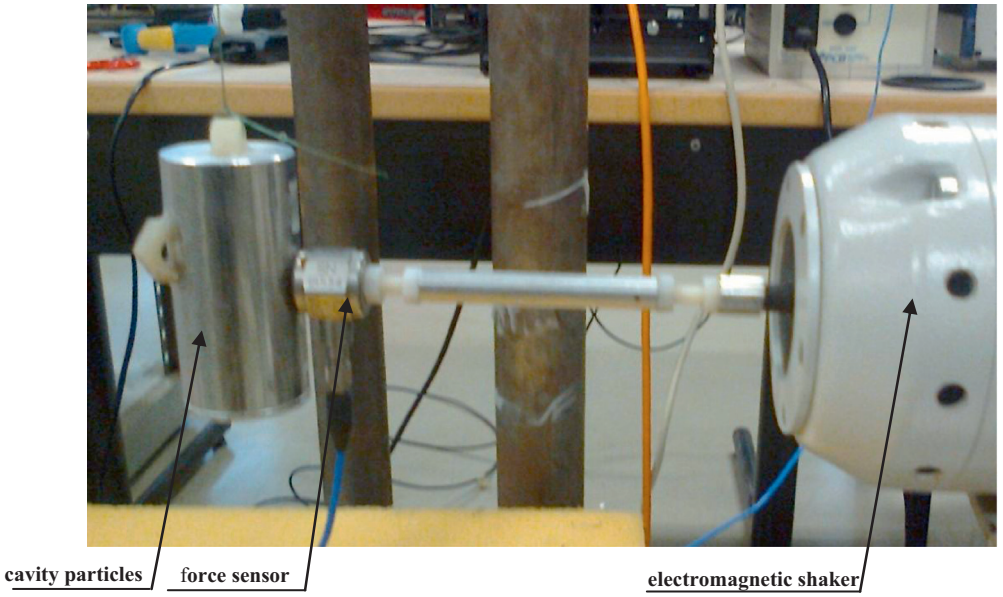

Fig. 3. Loss factor measurement setup (laser vibrometer not shown).

empty enclosure. It appears that these measurements are very sensitive to any phase error between force and velocity signals. Therefore the calibration step is of major importance.

2.3. Experimental results

The computation of active and reactive power was done using Eq. (3). Fig. 4 represents the variations of both dissipate and total power versus frequencies. These results were obtained for an enclosure having a diameter of 20×10^{-3} m and a length of 38×10^{-3} m. The computation of the loss factor was carried out using Eq. (4). Fig. 5 represents the variations of NOPD's loss factor versus frequency. The analysis of these results allowed us to note that compared to the loss factor of most structures which corresponds to 0.1, high values of loss factor were reached corresponding to 0.38, showing the efficiency of this passive process to drastically reduce vibration.

The curve of the loss factor can be explained by the mechanism of friction. The friction between particles from one hand and between the particles and the walls from the other dissipates the friction energy of the vibrating system. When the frequency level is quite low, the relative motion between particle–particle and particle–wall appears which results in a

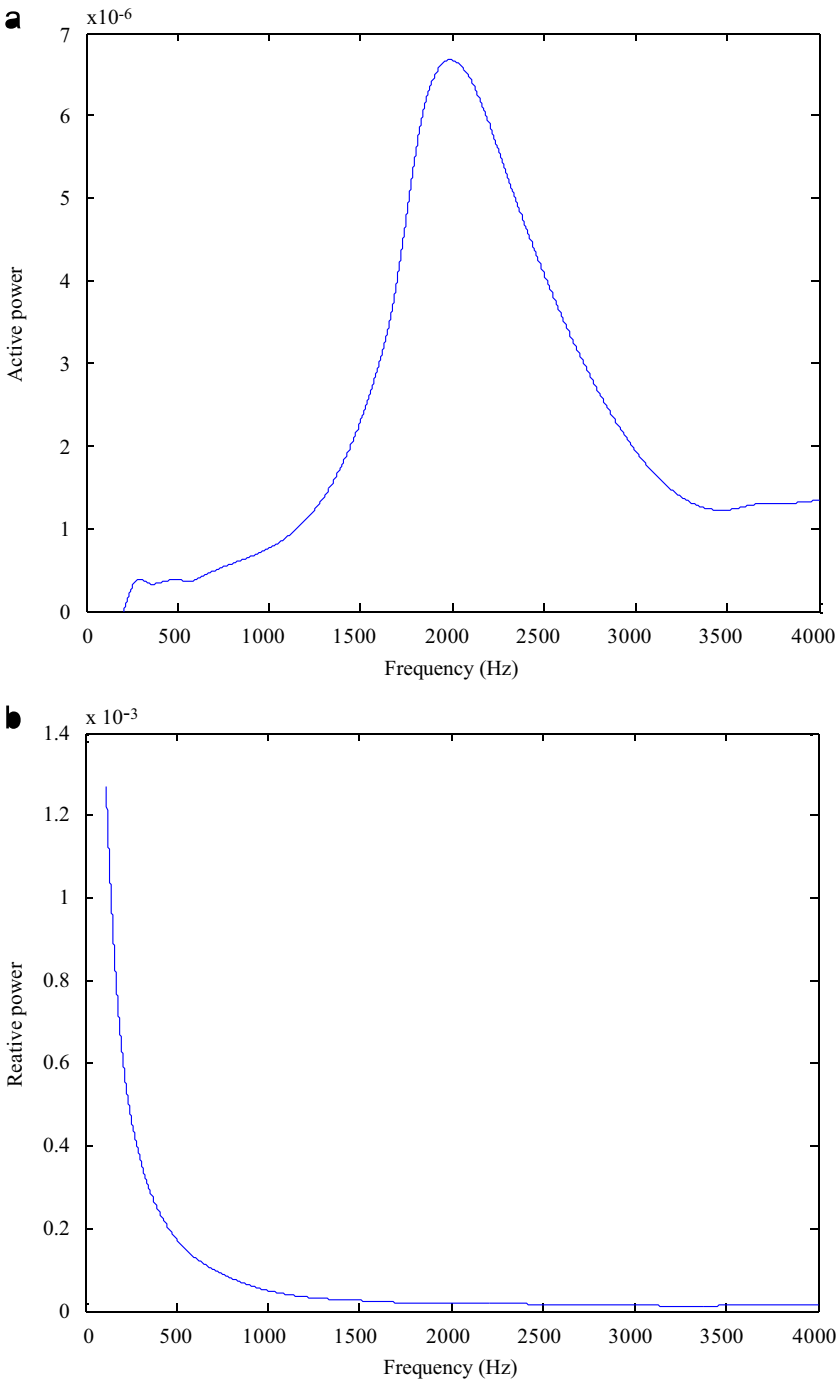

Fig. 4. (a) Active power versus frequency and (b) reactive power versus frequency.

small amount of dissipated energy and subsequently a relatively low loss factor. When the frequency level is increased, the motion of the granular particle becomes more agitated. These motions induce (cause) an increase in the dissipated energy by friction (Fig. 4) and subsequently a high value of the loss factor. With further increase in the frequency (as frequency increases), the particles tend to roll over one another reducing eventually the dissipated energy. Indeed, the granular friction interaction is substantially reduced which can be referred to as a decompaction phenomenon of the granular materials.

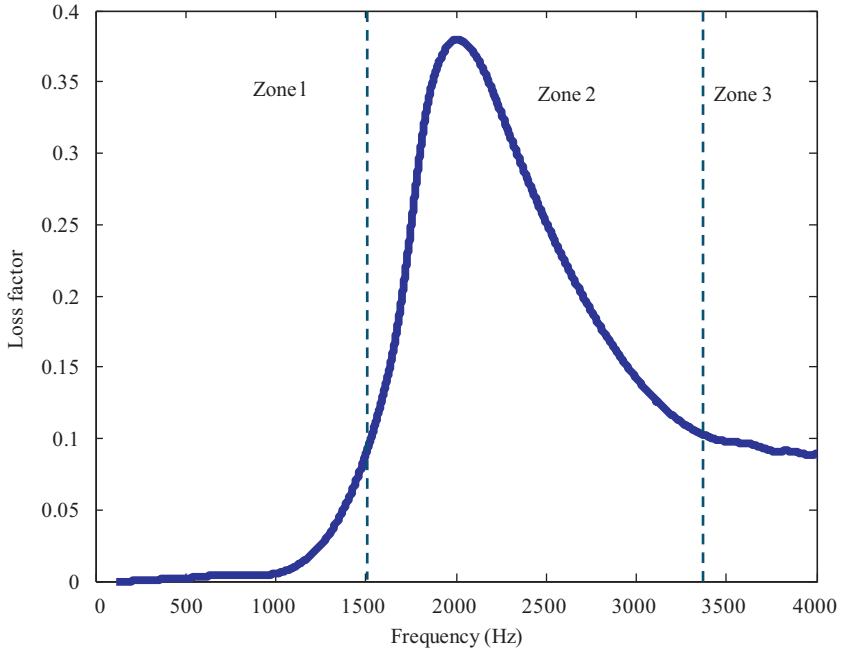

Fig. 5. NOPD loss factor versus frequency.

From this interpretation, two phenomena depending on the friction forces prevailing around the perimeter of the enclosure wall and between particles are distinguished. Indeed, if the enclosure is secured on an electromagnetic shaker delivering a sinusoidal excitation of amplitude $a\sin(\omega t)$, then the maximum value of the reduced acceleration will be $\Gamma = a\omega^2/g$ and the sheet of mass dm will then experience a force of intensity $\Gamma g dm$ opposed to its weight [19]. Then,

- if the reduced acceleration Γ imparted to the sheet is insufficient to overcome the forces of friction, the granular materials will remain compacted and no relative motion between them appears.
- In the opposite case, the sheet will be able to move, in case all upper sheets are also free to move, until eventually all the particles in the enclosure display a form of convective motion (the granular materials are said to undergo decompaction).

In short, sufficient accelerations obviously correspond to Γ greater than 1, for zones where the forces of friction exceed the force $\Gamma g dm$ and others where they are not expected to be formed. With these assumptions, the condition that allows a sheet to move freely with respect to the wall is simply

$$\Gamma g dm - g dm \geq dF_{friction}$$

where $g\,dm$ is the weight of the considered sheet. Its mass is given by $dm = \rho A dh$, where A is the area of the sheet and ρ its volumetric density. The elemental frictional force $dF_{friction}$ can be written as $dF_{friction} = k\mu_S p_v P dh$ which will be further detailed in Section 3.2.

This light interpretation of the loss factor curve will be continued by a dynamic model of the response in the future work of this research. So, I will take into account the dynamic effect presented in the research works [20,21].

The damper efficiency depends on several parameters (enclosure design, dynamics, etc.) [10] which are studied in the next section.

3. Parametric study

To reveal the influence of the damper parameters on the evolution of the loss factor, an experimental parametric study was conducted. The main studied parameters were

- the excitation levels and
- the enclosure design

3.1. Effect of the excitation levels on the loss factor evolution

Series of measurements was produced, with the same enclosure characteristic (diameter of 20×10^{-3} m and length of 38×10^{-3} m, steel particles), for different excitation levels. Fig. 6 shows the experimental variation of the loss factor versus frequency for eleven excitation levels. The analyses of these results indicated that the f_{max} of the loss factor shifted gradually with the increase of the enclosure's excitation. In addition, the loss factor is not very sensitive to this parameter compared to the frequency (Fig. 7).

Indeed, for a frequency of 700 Hz and with the increase of excitation level, the magnitude of the structure's velocity becomes more important (Fig. 8), which induces the increase of the local agitation of the particles in the enclosure. Then, the loss factor increases from 0.004 to 0.06. But, at frequencies beyond about 3000 Hz, the variation of the loss factor is less important (from 0.09 to 0.14).

Furthermore, there are two major mechanisms of energy dissipation: impact and friction damping between particles. The percentage of the intervention of these phenomena can explain the variation of the loss factor. For the lower excitation, the motion between particles is small; this would cause lesser friction energy. For the higher excitation level, the particles are more agitated which induces an increase in the number of small impact between them; as a result, the impact of energy dissipation will be added to the frictional dissipation and the level of the loss factor becomes more important.

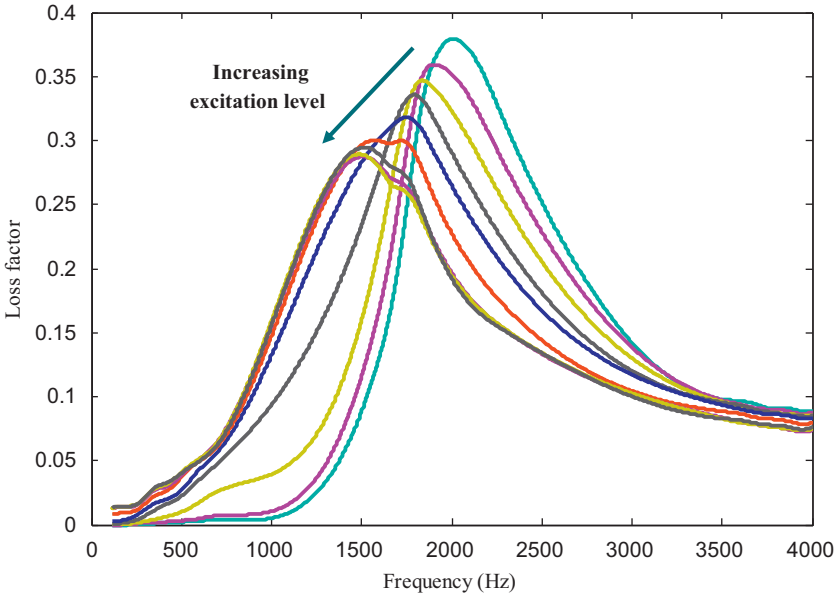

Fig. 6. NOPD loss factor versus excitation level.

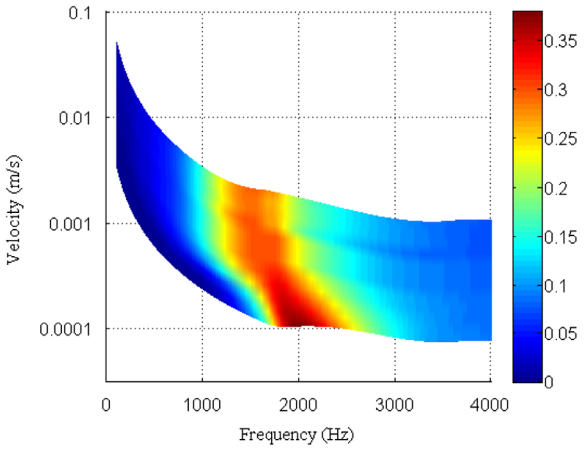

Fig. 7. NOPD loss factor versus velocity and frequency.

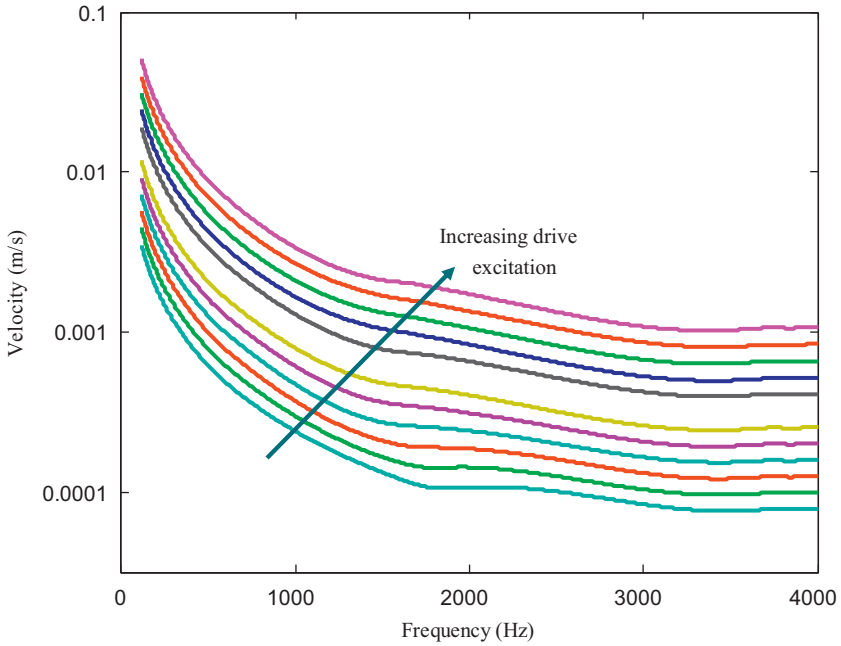

Fig. 8. NOPD velocity versus frequency.

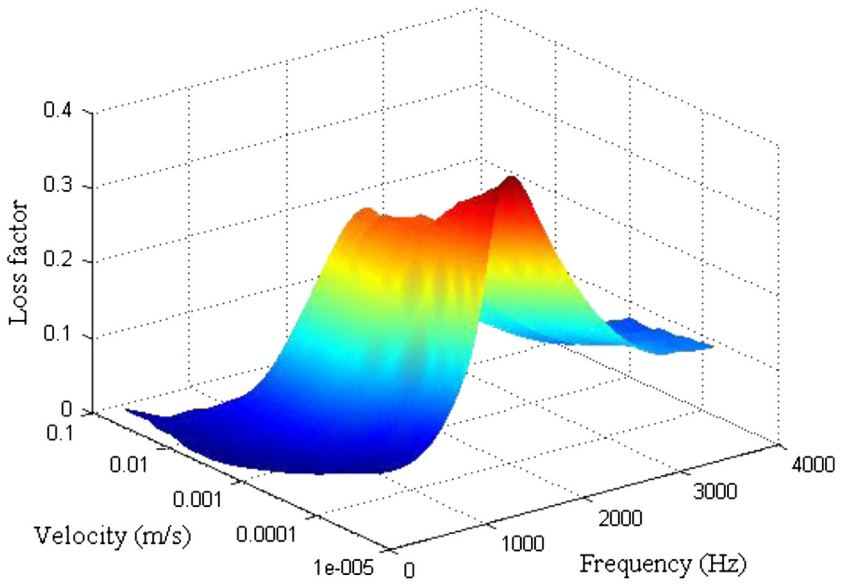

Fig. 9. NOPD loss factor.

Fig. 9 shows the evolution of the damping loss factor versus frequency and velocity measured during our experiment.

3.2. *Effect of the enclosure design on loss factor*

The performance of the NOPD depends on several parameters, such as pressure [10], particle size and frequency. In particular, the cavity design ($a=L/D$) is the most important parameter. In the two dimensional enclosure, this dimensionless number (L/D) characterises the distribution of forces between particles. With the same volume and same size of particles Liu et al. [13] tested five geometries on a SDOF (single degree of freedom) by comparing the FRFs (frequency response function). It can observed that the cavity geometry has an influence on the pressure static distribution in the cavity and then, on the movement of particle.

In order to study the effect of this parameter, we consider three different geometries of the enclosure ($d=0.5\times10^{-3}$ m). Table 1 and Fig. 10 describe the enclosure's dimensions.

The variation of the loss factor versus frequency shown in Fig. 11 corresponds to non-obstructive particle dampers geometries with a fixed level excitation. Comparing the different curves, it can be observed that the interior volume cavity has an important role in the dynamic behaviour of particle dampers. We can note that the enclosure presenting the most important value of $a=L/D$ leads to the highest level of f_{max}.

This experimental result can be interpreted by considering the relative magnitude of the static pressure acting between the layers of the particles in the enclosure.

Table 1
Designs of the enclosure used in the experimental studies.

Design of the enclosure	1	2	3
$a=L/D$	0.72	1	1.9
L (mm)	20	25	38
D (mm)	28	25	20
Particle cavity volume (mm^3)	12315	12271	11938
Mass of the enclosure (g)	131.7	121	136

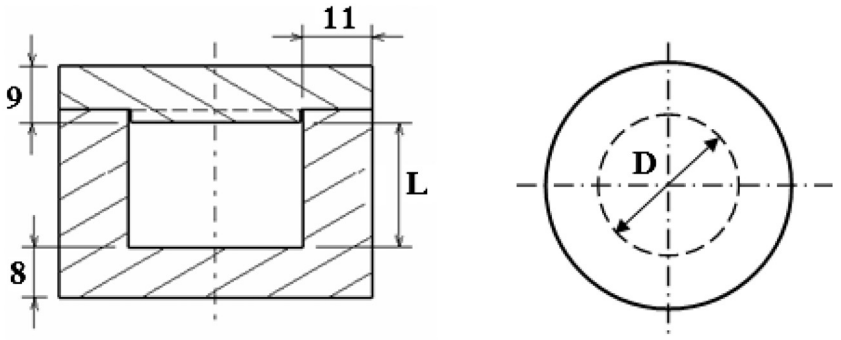

Fig. 10. Design of cavity (dimensions in mm).

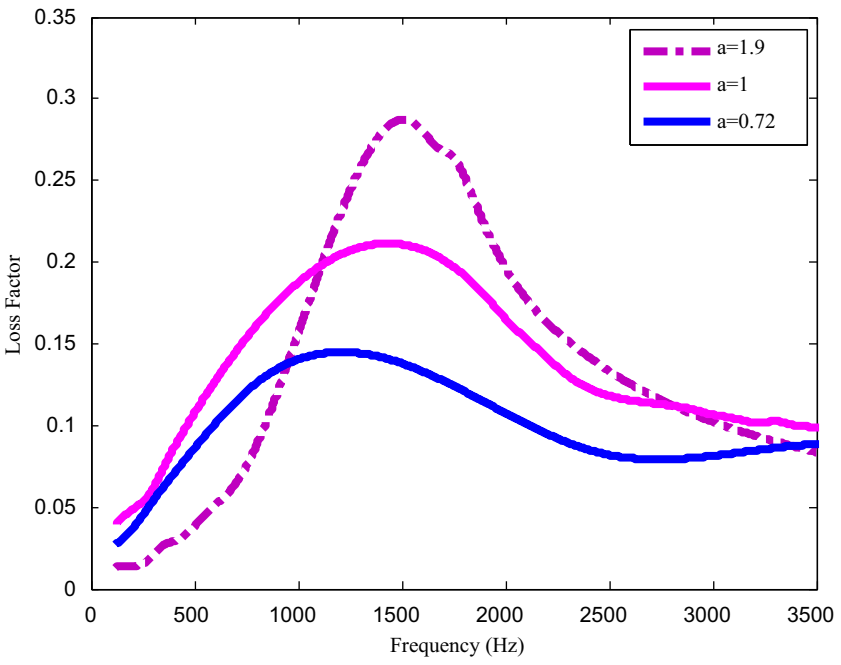

Fig. 11. NOPD loss factor for different enclosure designs.

Based on a standard procedure of powder mechanics, Janssen [18,19] proposed a heuristic model to calculate the static pressure for a vertical cylindrical container filled with granular particles.

Referring to Fig. 12, we consider a sheet of thickness dh situated at a height h in a cylinder of surface area A and perimeter P. Such a sheet is in equilibrium under the combined effect of several forces.

- Since pressure increases with depth, the slice of interest experiences a force directed toward the top and equal to Adp_v when p_v is the vertical pressure.
- The weight of a particle's layer of thickness dh constitutes a force directed toward the bottom and equal to $\rho\phi gAdh$, where ρ is the mass density of the material, which is assumed constant throughout the slice. And ϕ is the volume fraction expressed by this equation:

$$\phi = \frac{volume\ (particle)}{volume\ (total)} = \frac{N_p 4/3\pi R_p^3}{Ah} \tag{9}$$

  In these equations, N_p is the number of particles, R_p the radius of a particle (the particles are assumed to be identical and spherical), A the cross sectional area in squared metre (m^2) and h the height of the layer's particles i.e. $h=D_p=2R_p$.
- The force of friction at the walls results from infinitesimal movement of the granular particle's layer. Its value is equal to $\mu_S p_h Pdh$.

where p_v is the vertical pressure applied to the material which automatically generates a proportional horizontal pressure expressed as follows:

$$p_h = kp_v \tag{10}$$

where k is called the coefficient of redirection toward the wall of a vertical stress applied to the material. In the case of a compact triangular stack (Fig. 13), its value is approximately 0.58.

Taking into account (6), which related the horizontal and vertical components of the pressure, then, the friction forces are given by the following equation:

$$dF_{friction} = k\mu_S p_v Pdh \tag{11}$$

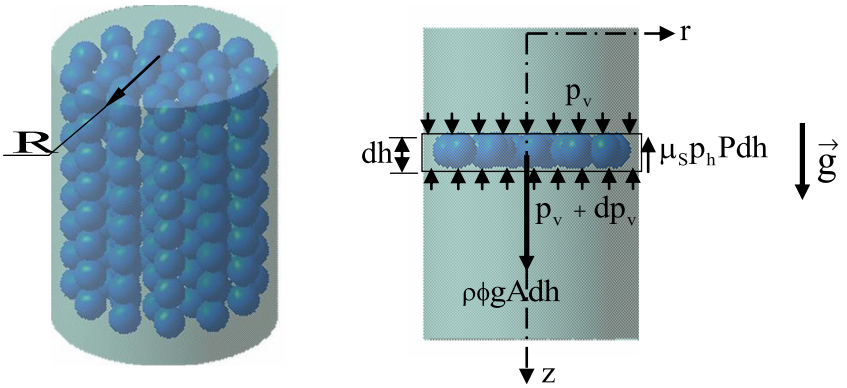

Fig. 12. Pressure distribution model.

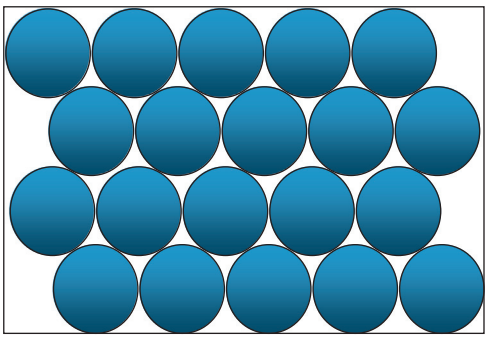

Fig. 13. Triangular lattice.

where μ_S is the static friction coefficient of the particles.

The equilibrium equation for the particular slice considered can be written as follows:

$$Adp_v + k\mu_S p_v P dh = \rho\phi g A dh \tag{12}$$

after division by dh and integrating the pressure, we obtain the equation:

$$p_v \exp\left(k\mu_S \frac{P}{A}h\right) = \rho\phi g \exp\left(k\mu_S \frac{P}{A}h\right) + C \tag{13}$$

where C is a constant which can be determined from initial conditions. Assume that p_{v0} is the initial pressure on the top of the structure, then Eq. (17) becomes

$$p_v = \frac{\rho\phi g A}{Pk\mu_S}\left[1 - \exp\left(-k\mu_S \frac{P}{A}h\right)\right] + p_{v0}\exp\left(-k\mu_S \frac{P}{A}h\right) \tag{14}$$

In the particular case where $p_{v0}=0$, the particles are in equilibrium under their own weight. Thus

$$p_v = \frac{\rho\phi g A}{Pk\mu_S}\left[1 - \exp\left(-k\mu_S \frac{P}{A}h\right)\right] \tag{15}$$

The trend of this case is illustrated in Fig. 14. Near the top of the structure, i.e. for $h \to 0$, the pressure goes as $p_v \approx \rho\phi g h$, which corresponds to the conventional hydrostatic pressure, similar to that applied by a column of water of depth h. The vertical pressure p_v saturates, as it approaches asymptotically a limit given by $p_v \to p_{sat} \to \rho g(A/Pk\mu_S)$, when $h \gg A/Pk\mu_S$.

It is noted that in the cylindrical Janssen model, Eq. (19) becomes

$$p_v = \frac{\rho f g D}{4k\mu_s}\left[1 - \exp\left(-\frac{4k\mu_s}{D}z\right)\right] = p_{sat}\left[1 - \exp\left(-\frac{4k\mu_s}{D}z\right)\right] \tag{16}$$

If we consider

$$\chi = (Ph/A)k\mu_S \tag{17}$$

Then referring to Eq. (20), the vertical pressure applied on a layer at that particular depth is equal to

$$p_v = \frac{1}{A}\frac{m\phi g}{\chi}(1 - e^{-\chi}) \tag{18}$$

where

$$\phi = \frac{2}{3}N_p\left(\frac{R_p}{R}\right)^2 \tag{19}$$

$$p_v = \left[\frac{2}{3A}\frac{mgN_p}{\chi}(1 - e^{-\chi})\right]\left(\frac{R_p}{R}\right)^2 \tag{20}$$

if it is assumed that the parameters in Eq. (16) are $\mu_s=0.74$ (steel to steel contact) [18], $k=0.58$, $\rho=7800\ \mathrm{kg/m^3}$, $\phi=0.58$ (measured for enclosure $a=1.9$). Fig. 15 indicates the evolution of the particles number versus normalised pressure distribution for the three enclosures considered. For a fixed number of particles, it can be seen that the enclosure

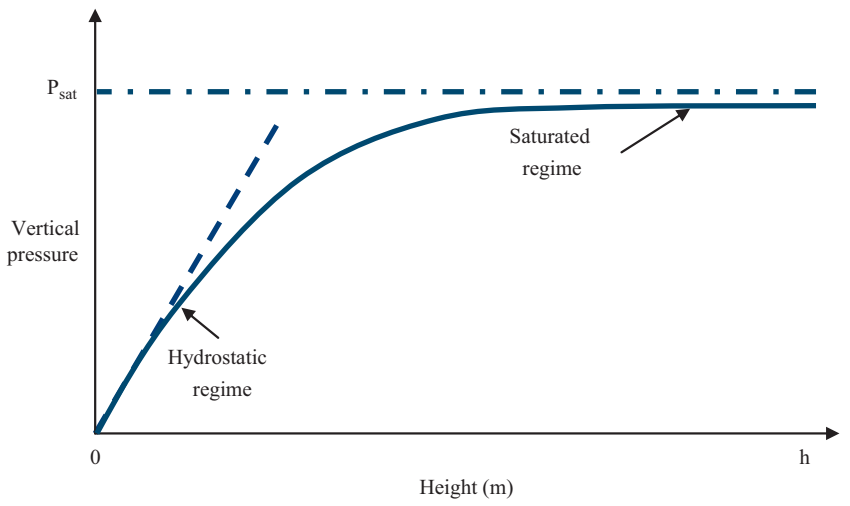

Fig. 14. Vertical pressure as a function of height.

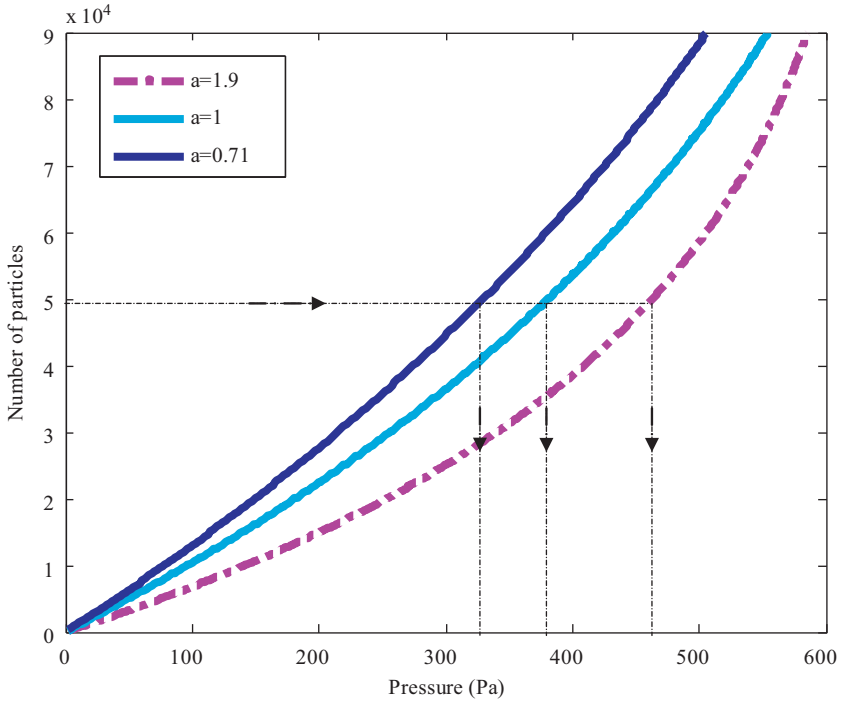

Fig. 15. Vertical pressure distributions for different enclosures.

with the largest diameter ($a=0.72$) presents the lowest value of the static pressure. This low static pressure applied on the particles makes their motion easier, allowing then the achievement of the f_{Max} value faster. This model can explain the loss factor evolution for different enclosure designs.

4. Investigation of a beam treated by NOPD

The aim of this section of our investigation is to predict the damping of a primary structure treated with NOPD using the loss factor characterised experimentally by the power method. An experimental study was conducted to compare experimental results with the simulation ones and to verify the capacity of the developed method to predict the dynamic behaviour of the primary structure treated with NOPD. The enclosure design presenting the highest loss factor and the least mass added is selected. Here, we consider the NOPD as a localised damping depending on the excitation frequency. The chosen vibrating structure is a free–free beam, which presents a bending eigenmode in the operating frequency band of the damper.

4.1. Experimental study

The experimental study (Fig. 16) consists of a primary structure and an enclosure (design: $a=1$), fixed in the middle of the beam, which contains steel particles. The material characteristics of the beam are mass density $\rho=7840\ \mathrm{kg/m^3}$, Young's modulus $E=2.1\times10^{11}$ Pa and Poisson ratio $v=0.33$. The beam dimensions are length $L=450\times10^{-3}$ m, width $l=40\times10^{-3}$ m and thickness $e=10\times10^{-3}$ m. The mass of the beam is 1.4 Kg. The steel particles have a diameter of 0.5×10^{-3} m and the total mass of the enclosure is 175.10^{-3} Kg. The beam is instrumented in free–free conditions. An electromagnetic shaker was used to provide a harmonic excitation force. The beam dynamic response is collected with a dynamic signal analyser: Siglab (Fig. 17). The location of the measurement point is chosen in order to describe adequately the dynamic response of the beam in the frequency band of interest [100–3000] Hz.

The modal characteristics are identified from the frequency response function (FRF). The identification results are presented in Table 2

Fig. 18 shows the frequency response function (acceleration/force) measured with and without particles. From this result, we can estimate the performance of the enclosure damper to reduce the vibratory level of the beam in its operating zone, where the loss factor is maximal (zone 2).

Furthermore, in the structure, the enclosure's location coincides with the antinodes vibrations. But, it is noted, in Table 2, that the presence of the particles causes an increase of the modal damping only for the third bending mode without significant changes of the natural frequencies of the structure. This result confirms that the dynamic response is reduced if the eigenfrequency is located in the operating frequency range of the enclosure dampers.

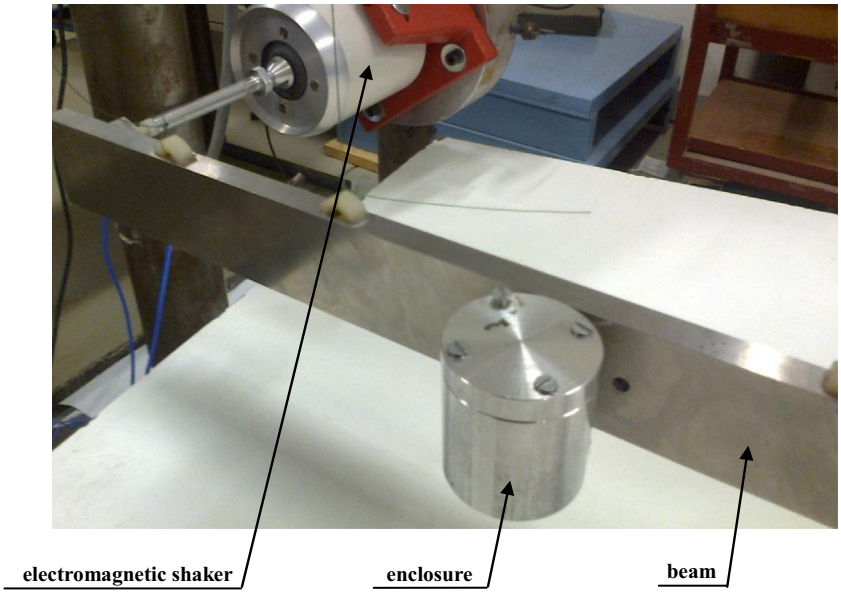

Fig. 16. Experimental process.

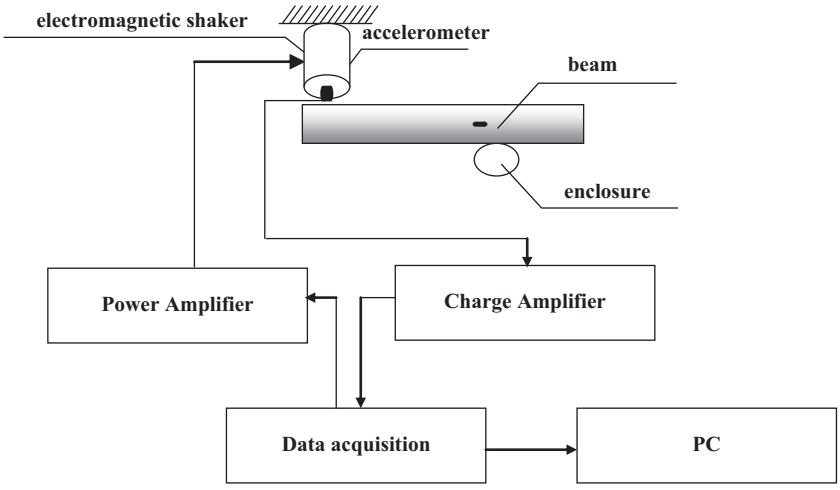

Fig. 17. A schematic of experiment setup.

Table 2
Experimental eigenfrequencies of the beam with and without the damper holes.

Mode no.	Without particles		With particles	
	Frequency (Hz)	Modal damping (%)	Frequency (Hz)	Modal damping (%)
1	264.4	0.014	258.9	0.053
2	765	0.16	766.2	0.19
3	1388.8	0.17	1364.1	2.1
4	2513.1	0.42	2511	0.41

4.2. Numerical study

In this section, the loss factor of NOPD which was determined experimentally is converted into an equivalent viscous damping. The latter can be easily used in the dynamic prediction model. The contribution of NOPD is estimated as an equivalent linear viscous damping coefficient $c(\omega)$ determined for different levels of the excitation frequency.

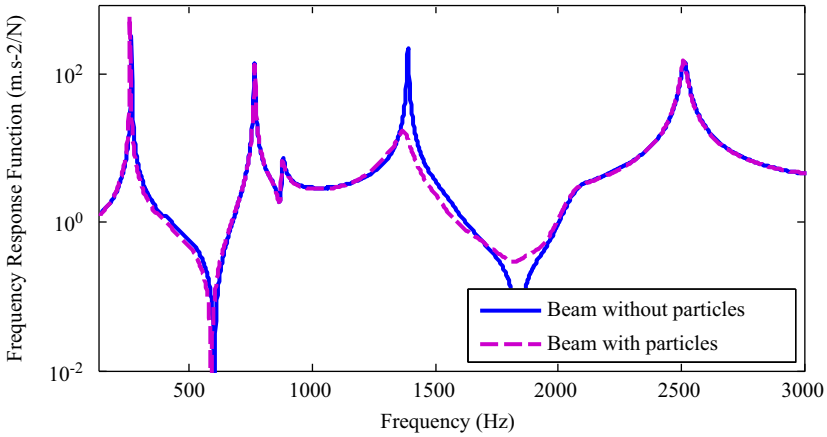

Fig. 18. Experimental FRF of the beam with and without the particles.

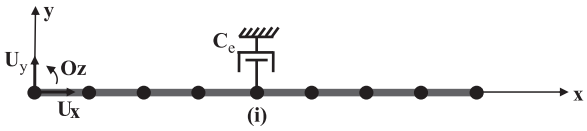

Fig. 19. Beam FEM model.

If we consider that the system is constituted by the enclosure mass m_e and the particles mass m_p. Then the motion equation can be expressed by

$$(m_e+m_p)\ddot{x}(t)+c(\omega)\dot{x}(t)=f(t) \tag{21}$$

where $c(\omega)$ is an equivalent linear viscous damping coefficient and $f(t)$ represents the excitation force.

For the harmonic excitation, when ω is the excitation frequency, the equation becomes

$$-\omega^2(m_e+m_p)x(\omega)+jc(\omega)x(\omega)=F(\omega) \tag{23}$$

and the power of the damped system can be expressed by

$$P(\omega)=\frac{1}{2}\left(\frac{F^2(\omega)c(\omega)}{-(c(\omega))^2-\omega^2(m_e+m_p)^2}+j\frac{\omega F^2(\omega)(m_e+m_p)}{-(c(\omega))^2-\omega^2(m_e+m_p)^2}\right) \tag{24}$$

Then, using Eqs. (22) and (4), the loss factor is computed by

$$\eta(\omega)=\frac{c(\omega)}{\omega(m_e+m_p)} \tag{25}$$

Finally, the loss factor characterised experimentally will be converted into an equivalent linear viscous damping depending on the excitation frequency

In the second step, the aim of the numerical simulation is to predict the response of a primary structure treated with NOPD using the damping coefficient characterised experimentally by the power method. Fig. 19 shows a schematic of the adopted model treated with NOPD. The beam is modelled by the finite element method using 2-D beam elements. The NOPD is modelled by equivalent frequency dependent viscous damping.

The equilibrium equation of the structure can be expressed by

$$[M]\{\ddot{x}\}+[C(\omega)]\{\dot{x}\}+[K]\{x\}=\{f\} \tag{26}$$

where {X}, {f} and [K] represent respectively the nodal displacement of the beam, the external force applied to the structure and the stiffness matrix. [M] is the mass matrix of both the beam and the enclosure with the particles located at the node (i).

$$[M]=[M_b]+[M_a] \tag{27}$$

where $[M_b]$ and $[M_a]$ are respectively the mass matrix of the beam and the additional mass matrix.

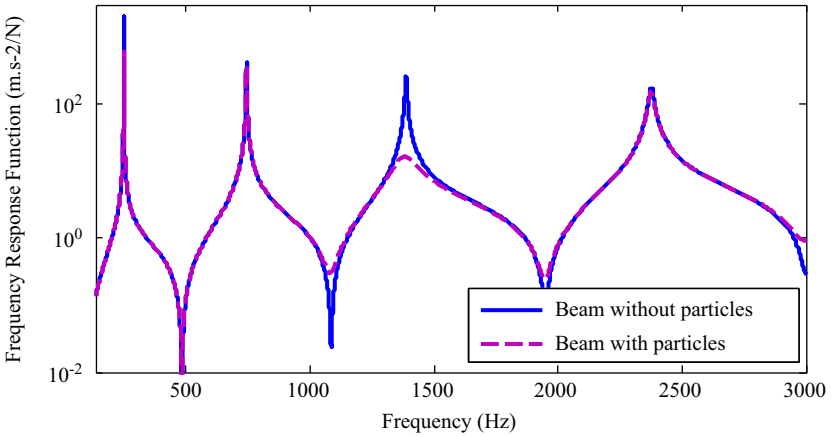

Fig. 20. Numerical FRF of the beam with and without the particles.

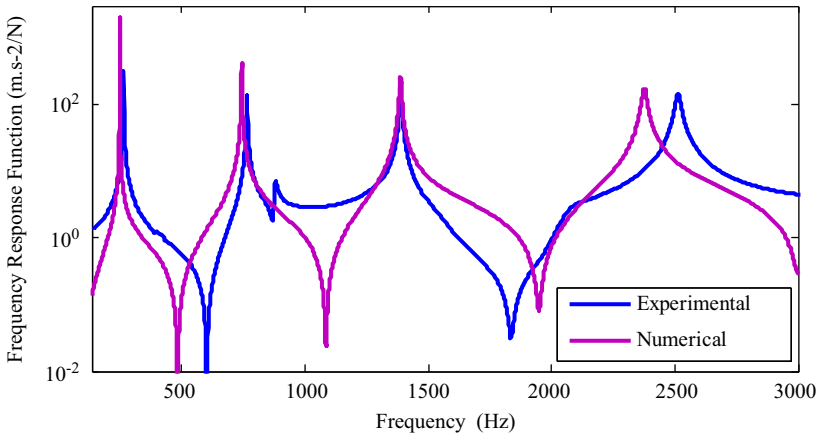

Fig. 21. Experimental and numerical FRFs of the beam without the particles.

We note also $[C(\omega)]=[C_0(\omega)]+[C_v(\omega)]$ the damping matrix of the global structure, where $[C_0(\omega)]$ is the proportional damping matrix of the beam and $[C_v(\omega)]$ represents the additional damping matrix carried by the particles.

$$[C_v(\omega)] = i \begin{bmatrix} & & i & & \\ 0 & & \vdots & & 0 \\ & \ddots & \vdots & & \\ \cdots & \cdots & c_e(\omega) & \cdots & \cdots \\ & & \vdots & \ddots & \\ 0 & & \vdots & & 0 \end{bmatrix} \tag{28}$$

$c_e(\omega)$ is the equivalent localised viscous damping of the experimental NOPD.

The implementation of this modelling was performed in a MATLAB environment.

Fig. 20 shows the calculated frequency response function of the beam with and without the effects of NOPD. It is noticed that the NOPD can reduce the dynamic response of the third frequency of the structure which is in agreement with the experimental results (Fig. 18).

Figs. 21 and 22 show a comparison between numerical and experimental FRFs for two configurations (with and without particles). It appears that the modal damping effect is correctly predicted by the proposed model in the operating frequency band of the damper.

5. Conclusions

The study proposed in this paper aimed at finding novice ways to ameliorate the characterisation of the NOPD behaviour independently of the vibrating structure. Due to a large number of dynamic parameters, a simple and effective experimental method was presented. The instantaneous experimental measurement of force and velocity allowed the

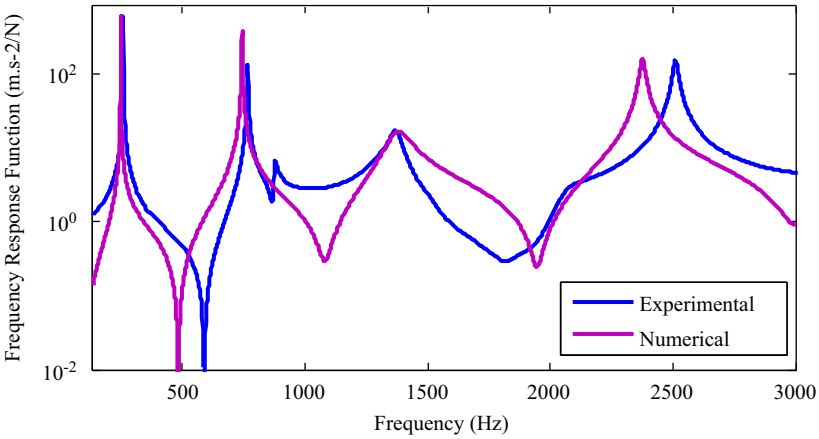

Fig. 22. Experimental and numerical FRFs of the beam with the particles.

identification of the loss factor in different designs of dampers. The friction particle damping is believed to be remarkably effective. Although it is a non-linear behaviour, a strong rate of energy dissipation is achieved within a broadband frequency range.

The non-obstructive particle damper characterised experimentally will be converted into an equivalent viscous damping depending on the excitation frequency. The numerical and experimental studies of a beam treated by NOPD were performed in order to verify that the loss factor identified by power measurements enabled us to predict the dynamic behaviour of the vibrating structure. The results obtained show that the proposed characterisation and model prediction can be generalised and used to reduce vibration response of more complex mechanical structures.

The optimal damping effect might be achieved by using a design of different types of particle enclosure involving an appropriate combination of friction and shear phenomena. Our future research will be focused on the development of a dynamic model of the loss factor response.

References

[1] Ameur Chettah, Vibroacoustic Behaviour of Structures Constructed From Recycled Tire Crumb, Ph.D. Thesis (in French), University of Reims, Ecole Centrale de Lyon, France, 2008.
[2] Z.W. Xu, M.Y. Wang, T.N. Chen, Particle damping for passive vibration suppression: numerical modelling and experimental investigation, J. Sound Vib. 279 (3-5) (2005) 1097–1120.
[3] Z.W. Xu, M.Y. Wang, T.N. Chen, An experimental study of particle damping for beams and plates, J. Vib. Acoust. Trans. ASME 126 (1) (2004) 141–148.
[4] A. Papalou, S.F. Masri, An experimental investigation of particle dampers under harmonic excitation, J. Vib. Control 4 (1998) 361. 179.
[5] K.S. Marhadi, V.K. Kinra, Particle impact damping: effect of mass ratio, material, and shape, J. Sound Vib. 283 (2005) 433–448.
[6] R.D. Friend, V.K. Kinra, Particle impact damping, J. Sound Vib. 233 (1) (2000) 93–118.
[7] M. Saeki, Impact damping with granular materials in a horizontally vibrating system, J. Sound Vib. 251 (1) (2002) 153–161.
[8] J.J. Moore, A.B. Pallazzolo, A forced response analysis and application of impact damper to rotordynamic vibration suppression in a cryogenic environment, J. Vib. Acoust. 117 (1995).
[9] A.L. Paget, Vibration in steam turbine buckets and damping by impacts, Engineering 143 (1937) 305–307.
[10] Lenzi A., The Use of Damping Material in Industrial Machines, Ph.D. Thesis, University of Southampton, 1982.
[11] H.V. Panossian, Structural damping enhancement via non-obstructive particle damping technique, J. Vib. Acoust. 114 (1992) 101–105.
[12] Bourinet J.M. Numerical and Experimental Studies of Damped Vibrations of Tubes Filled With Granular Materials, Ph.D. Thesis, Ecole Centrale de Nantes, 1996, (in French).
[13] W. Liu, G.R. Tomlinson, J.A. Rongong, The dynamic characterisation of disk geometry particle dampers, J. Sound Vib. 280 (3–5) (2005) 849–861.
[14] Z.W. Xu, M.Y. Wang, T.N. Chen, A particle damper for vibration and noise reduction, J. Sound Vib. 270 (4-5) (2004) 1033–1040.
[15] J. Park, D. Palumbo, Damping of structural vibration using lightweight granular materials, Exp. Mech. 49 (2009) 697–705.
[16] M.Y. Yang, Development of Master Design Curves for Particle Impact Dampers, Ph.D. Thesis, The Pennsylvania State University, 2003.
[17] C.X. Wong, M.C. Daniel, J.A. Rongong, Energy dissipation prediction of particle dampers, J. Sound Vib. (2009) 91–118.
[18] M.E. Fayed, L. Otten, Handbook of Powder Science and Technology, 2nd ed. Chapman & Hall, New York, 1997.
[19] J. Duran, Sands, Powders, and Grains: An Introduction To the Physics of Granular Materials, Springer, Berlin, 1999.
[20] A. Carcaterra, A. Akay., C. Bernardini, Trapping of vibration energy into a set of resonators: theory and application to aerospace structures, Mech. Syst. Signal Process. 26 (2012) 1–14.
[21] N. Roveri, A. Carcaterra, A. Akay, Vibration absorption using non-dissipative complex attachments with impacts and parametric stiffness, J. Acoust. Soc. Am. 126 (5) (2009) 2306–2314.